Influence of the Ceramide(III) and Cholesterol on the Structure of a Non-hydrous Phospholipid-based Lamellar Liquid Crystal : Structural and Thermal Transition Behaviors

Tae Hwa Jeong[†] and Seong-Geun Oh[*]

Department of Chemical Engineering, Hanyang University, Seoul 133-791, Korea. [*]E-mail: seongoh@hanyang.ac.kr
[†]Skin Research Institute, Korea Kolmar Corporation, Yeongi-Gun, Chung-Nam 339-851, Korea
Received February 21, 2007

The effects of the creamide III (CER3) and cholesterol (CHOL) on the structure of a non-hydrous distearoyl phosphatidylcholine (DSPC)-based lamellar liquid crystal (LC) hydrated by only propylene glycol (PG) without water were investigated by differential scanning calorimetry (DSC), X-ray diffractions (XRDs), and polarized microscope (PM). As soon as CER3 was incorporated into the lamellar phase, the characteristic LPP was appeared as well as the characteristic SPP, and the formation of separated CER3 crystalline phase was observed depending upon the increase of CER3 content by XRDs. Also, by DSC, it was shown that the increase of CER3 made the monotectic thermal transition be changed to the eutectic thermal transition which indicates the formation of separated CER3 crystalline phases and the main transition temperatures (T_{c1}) to be gradually decreased and the enthalpy change (ΔH) to be linearly increased. Incorporating CHOL, the formation of LPP and SPP showed almost similar behaviors to CER3, but incorporating small amounts of CHOL showed the characteristic peaks of CHOL which meant the existence of crystalline CHOL phase due to the immiscibility of CHOL with DSPC swollen by PG differently from CER3, and increasing CHOL made the intensity of the 1st order diffraction for LPP weakened as well as the intensities of the characteristic diffractions for DSPC. Also, in the results of DSC, it showed more complex thermal behaviors having several T_c than CER3 due to its bulky chemical structure. In the present study, the inducement of CER3 and CHOL as other lipids present in human stratum corneum (SC) into a non-hydrous lamellar phase is discussed in terms of the influence on their structural and thermal transition.

Key Words : Ceramide III, Cholesterol, Distearoylphosphatidylcholine, Non-hydrous, Lamellar

Introduction

Transdermal administration is limited by the stratum corneum (SC), the outer layer of skin, considered as the main barrier to percutaneous absorption of drugs. The SC is composed of keratin-filled dead cells which are entirely surrounded by crystalline lamellar lipid regions having a very dense structure.[1]

The natural function of the skin is the protection of the body against the loss of endogenous substances such as water as well as against an undesired influence from the environment caused by exogeneous substances. Therefore, when most of active substances applied onto the skin diffuse along the crystalline lamellar lipid layer in the intercellular region, this dense structure obstructs the diffusion of active substances, reduces the efficiency of drug delivery into skin, and decreases the desirable effects such as whitening, anti-wrinkle, or moisturizing etc.[2]

Phospholipids are a potential group of penetration enhancers and have been administered as safe.[3] Being composed of natural body constituents and being biodegradable, phospholipids have been very useful in the cosmetic and pharmaceutical industry as unique natural and biocompatible emulsifiers.[4,5] Also, drug penetration can be more increased in the case of some combination of phospholipids and low molecular weight of polar solvents which efficiently decrease the barrier resistance of the stratum corneum (SC).[6,7] Mainly in pharmaceutical fields, numerous studies have evaluated the percutaneous penetration of some active substances such as testosterone, haloperidol, flurbiprofen etc using various penetrating enhancers such as propylene glycol (PG), polyethylene glycol (PEG), their derivatives, ethyl alcohol, glycerol monooleate, and so on.[8-11]

In the previous study, we have investigated a skin model membrane having non-hydrous lamellar crystalline structure with DSPC as a main lipid and propylene glycol (PG) as a polar solvent and confirmed that it is possible to make a non-hydrous lamellar structure and PG molecules swell the DSPC-based lamellar structure by the interaction with both polar region and non-polar region.[12] This non-hydrous lamellar crystal might be very useful to stably encapsulate some important active substances such as retinoids, ubiquinones, tocopherols by avoiding the contact with water molecules and protecting from their oxidization. Also, there are ceramides and cholesterol among the most important lipids in SC. They form the 'mortar' region responsible for the barrier function of the skin and having dense lamellar crystalline structure in the unique structure model, 'brick and mortar', suggested by Elias *et al.*[13] The composition of this skin model membrane different from other biomem-

Table 1. Lipid composition [%(w/w)] of human SC investigated from different references

The class of lipids	1983 (Lampe *et al.*)	1990 (Elias, P.M.)	1996 (Wertz, P.W.)
Ceramides	18.1	35	50
Cholesterol	14	20	25
Free fatty acids	19.3	25	10.0~15.0
Triglycerides	25.2	Trace	Trace
Sterolesters	5.4	10	5
Other	18	10	–

branes, since a phospholipid, which is absent in SC, is used as a polar lipid mainly forming bilayers and mixed with the main class of neutral lipids such as a ceramide and cholesterol with an ordered multi-lamellar structure.[14] These compositions were quantitatively investigated by the extraction method and the solvent, the pre-treatment of solvent and inter- and intra-individual variations.[15-17] Table 1 summarizes the compositions from different references.

As seen in Table 1, the major part of SC lipids are ceramides and they are the most important component of the SC multi-lamellar lipid structure with distinct physiochemical properties necessary for the barrier function of the skin. The other major lipids are cholesterol and long-chain free fatty acids. Nine different extractable ceramides have been detected in human SC, which are classified as CER1 to CER9.[18-21] The CER can be subdivided by three main groups, based on the nature of their head group architectures [sphingosine (S), phytosphingosine (PS) or 6-hydroxysphingosine (HS). Through an amide bonding, long-chain non-hydroxy (N) or α-hydroxy (A) fatty acids with varying acyl chain lengths are chemically linked to the sphingosine bases. In Figure 1, the molecular structures of CER together with the two nomenclatures are illustrated.

Another major lipid, CHOL, have the effect seen through its impact on other components, such as the broadening and modulation of phase transitions in phospholipids membranes.[22,23] These effects are evident in ceramide/fatty acid/cholesterol SC lipid system.[24]

The structural and thermal transition behaviors to influence of the creamide III (CER3) and cholesterol (CHOL) on the structure of a non-hydrous distearoyl phosphatidylcholine (DSPC)-based lamellar liquid crystal hydrated by only propylene glycol (PG) without water were examined by differential scanning calorimetry (DSC), X-ray diffractions (XRDs), and polarized microscope (PM). In this paper, we chose two human SC lipids which are CER3 among 9 types of CER and cholesterol to be more similar structure to human SC and have better skin affinity, and then investigated their influence on a non-hydrous DSPC-based lamellar structure with DSC, small angle X-ray diffraction (SAXD), wide angle X-ray diffraction (WAXD), and PM.

The aim of this work is to better understand the structural and thermal transition behaviors of non-hydrous LC influenced by CER 3 which is widely used in cosmetics among various kinds of ceramides and CHOL, and apply them to cosmetics and pharmaceutics afterward in order not only to repair the defected skin barrier and increase the efficiency of their drug delivery into skin, but also to stably encapsulate active substances mentioned above.

Materials and Methods

Materials. DSPC as a phospholipid was purchased from Lipoid (Germany), a ceramide (CER3, 95.0%>) was purchased from Doosan biotech (Korea), a cholesterol (CHOL, 99.0%>) was purchased from Solvay (U.S.A), and PG was purchased from Merck (Germany). All of the materials were used as commercial grades and without any pre-treatment.

Methods

Sample preparation: At first, DSPC, CER3, and CHOL were added to PG as a solvent under a moderate agitation. This mixture was heated to 80 °C and was continuously agitated until being completely melted. This melted mixture was cooled to 60 °C with a moderate cooling speed, and

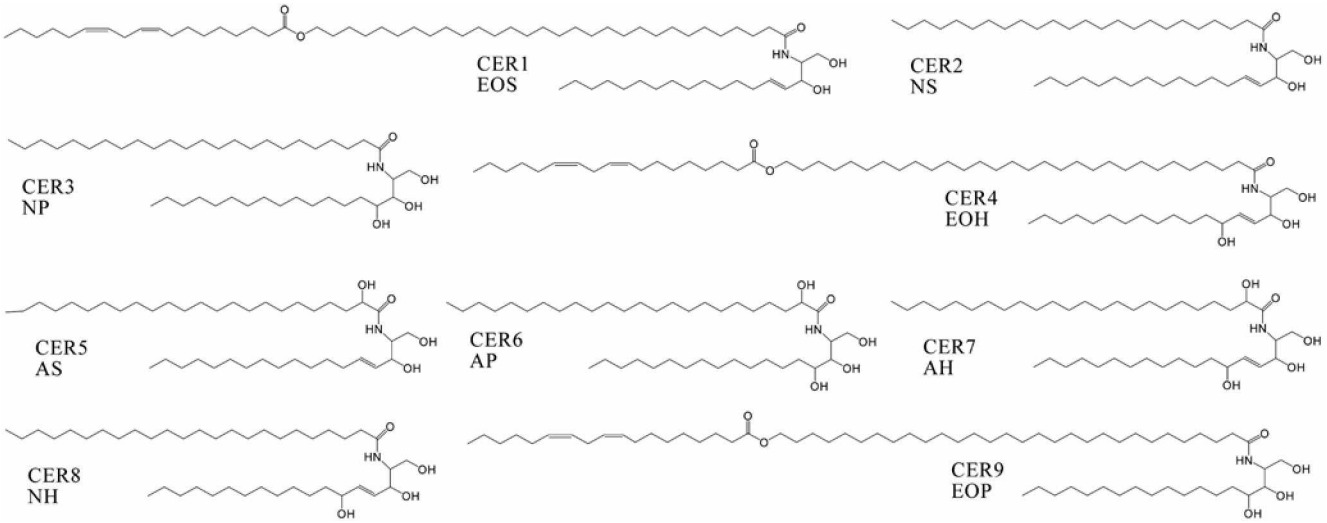

Figure 1. The molecular structures of the CER present in human SC.

then was very slowly cooled to 35 °C and stored below 10 °C for 1 week before being analyzed.

DSC analysis: Thermal analysis was performed with a TA instrument (TA4100 model) from 20 °C to 120 °C for CER3 and from 20 °C to 150 °C for CHOL at heating rate of 2 °C/min after being cooled to a lower temperature. Sample quantities were about 10 mg, which was sealed in an aluminum sample cell. This analysis was done under a nitrogen gas and was observed the phase transition temperature (T_c) and enthalpy change (ΔH) at the temperature to confirm the formation of LC structure and its thermal transition during heating process.

XRD analysis: XRD spectra were taken with XDS 2000 model (SCINTAG INC., USA). During this experiment the temperature of the samples deviated by maximum 1 °C from the adjusted temperature (24 °C). XRD experiments were carried out with Ni-filtered CuK α-ray (λ = 1.54 Å) using photo detection. SAXS data were recorded using a position sensitive proportional counter with a camera length of 350 mm and associated electronics (multichannel analyzer, etc. SCINTAG INC., USA).

The scattering intensity was measured as a function of scattering vector, q. The scattering vector is defined as $q = (4\pi/\lambda)\sin\theta$, where 2θ is the scattering angle and λ is the X-ray wavelength (1.54 Å). The lamella repeat distance, D, was calculated as an average from the first and second order of diffraction according to $D = 2\pi/q_1$ for the first order of diffraction peak and $D = 4\pi/q_2$ for the second order of diffraction peak by following the same way as J. Zbytovska *et al.*[25]

WAXS patterns were recorded by a flat-plate film cassette loaded with a high-sensitive X-ray film (Fuji Medical X-ray Film) with a camera length of 66.0 mm. Samples were sealed in a thin-walled glass capillary tube (outer diameter 1.0 mm) and mounted in a thermostable holder whose stability was ± 0.2 °C.

PM analysis: All lipid mixtures were examined with an Olympus BX-51 polarized microscope using crossed polarizers at 24 °C ± 1 °C below overall transition temperature (T_c).

Results and Discussion

The micro-structural variances of the model matrices depending on the CER3 contents at a fixed 20 wt% of DSPC

Structural transitions corresponding to the increase of CER3 by XRDs: Figure 2 shows the small angle X-ray diffraction (SAXD) patterns for DSPC only and its complex with PG. The influence of PG induced into DSPC lamellar phase has ever been investigated in the previous study[12] and it showed that the inducement of PG remarkably decreased the intensity of the 1st order diffraction due to the action as a solvent for the stearyl group of DSPC differently from water molecules and made the bilayer distance (D) be longer, but the extension of D value was shown to be relatively smaller in comparison with water molecules. As seen in Figure 2,

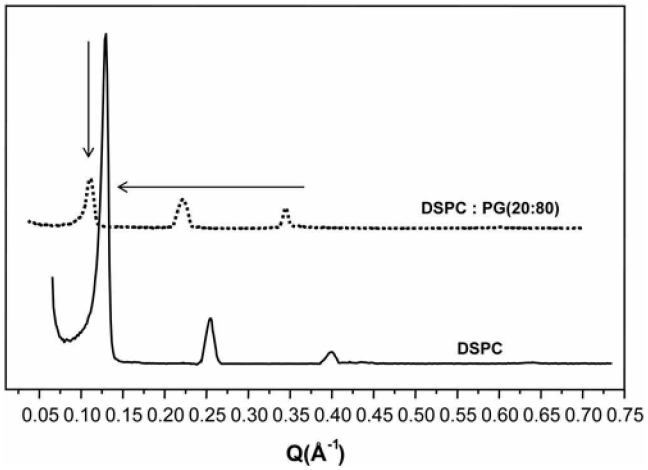

Figure 2. Small angle X-ray diffraction patterns for DSPC itself and its complex swollen by an excess of PG.

DSPC showed the diffraction pattern for the 1st, 2nd, and 3rd order at q = 0.130 Å^{-1}, 0.254 Å^{-1}, 0.396 Å^{-1} and its bilayer distance was calculated as 48.33 Å which is slightly higher than the theoretical value (46.8 Å), but the inducement of PG into DSPC made the diffraction pattern shifted to left side and its bilayer distance was calculated as 56.25 Å as well as the dramatic decrease of the intensity.

Experimentally, CER3 to be used in this study showed the SAXD pattern to have two coexisting crystalline lamellar phase: one is represented as long periodicity phase (LPP) at q = 0.07, 0.141 Å^{-1} and another is represented as short periodicity phase (SPP) at q = 0.165, 0.33, 0.493 Å^{-1}. And the distance for LPP was calculated as 89.7 Å and the distance for SPP was calculated as 38.06 Å. Interestingly, the formation of the characteristic LPP appeared as soon as CER3 was induced in the DSPC/PG lamellar phase as well as the characteristic SPP, similarly to native SC which can be expressed by two coexisting crystalline lamellar phase: the LPP with a periodicity of approximately 13 nm and the SPP

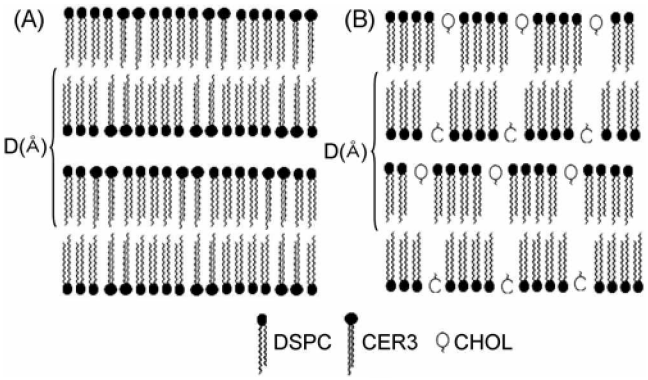

Figure 3. Schematic representation of lamellar crystalline phases based on the DSPC/CER3 (A) and DSPC/CHOL (B) when complexed with a polar solvent. Lipid headgroups are represented by black circles (DSPC and CER) attached to two hydrocarbon chains and by a blank circle (CHOL) attached to a short hydrocarbon chain. The D value is the ordinate for the repeating distance in lamellar structure.

with a periodicity of approximately 6 nm.[26]

As seen in Figure 3, CER3 has a very similar molecular structure to DSPC, while it has a high crystallinity. In Figure 4, it was shown that the incorporation of CER3 into DSPC lamellar phase made the overall structural transitions (Fig. 4(A)) in the measuring range and the regional transition patterns (Fig. 4(B)) in q values from 0.2 to 0.75, dependently on increasing CER3 contents with SAXD.

In the range of CER3 content up to 2 wt%, there were two peaks representing for LPP at q = 0.042 $Å^{-1}$, 0.085 $Å^{-1}$, and the distance of LPP at these q values was calculated as approximately 148.63 Å which was much longer than CER3 itself due to the formation of the homogeneous lamellar structure being composed of DSPC and CER3. In this range, there were three peaks representing for SPP at q = 0.12 $Å^{-1}$, 0.24 $Å^{-1}$, 0.36 $Å^{-1}$ and the distance of SPP at these q values was calculated as approximately 52.13 Å which was slightly shorter than DSPC swollen by PG, but, as seen in Figure 4, there were no characteristic peaks for separated CER3 crystalline phases and it was confirmed that DSPC and CER3 formed the homogeneous lamellar phase due to their similar structures in the presence of PG without water.

However, from 3 wt% of CER3, other peaks appeared in the region of q = 0.16 $Å^{-1}$, 0.33 $Å^{-1}$, 0.49 $Å^{-1}$ almost same as CER and the intensities of these peaks significantly elevated depending on the increase of CER3 content in Figure 4. It suggests that another phase in DSPC-CER3 lamellar phase was progressed to appear and this phase can be ascribed to the crystalline CER3 in a V-shaped structure due to its high crystallinity.[27]

As seen in Figure 5, DSPC showed four characteristic peaks at 2θ = 4.3°, 5.72°, 8.6° and 21.24° and the last peak at

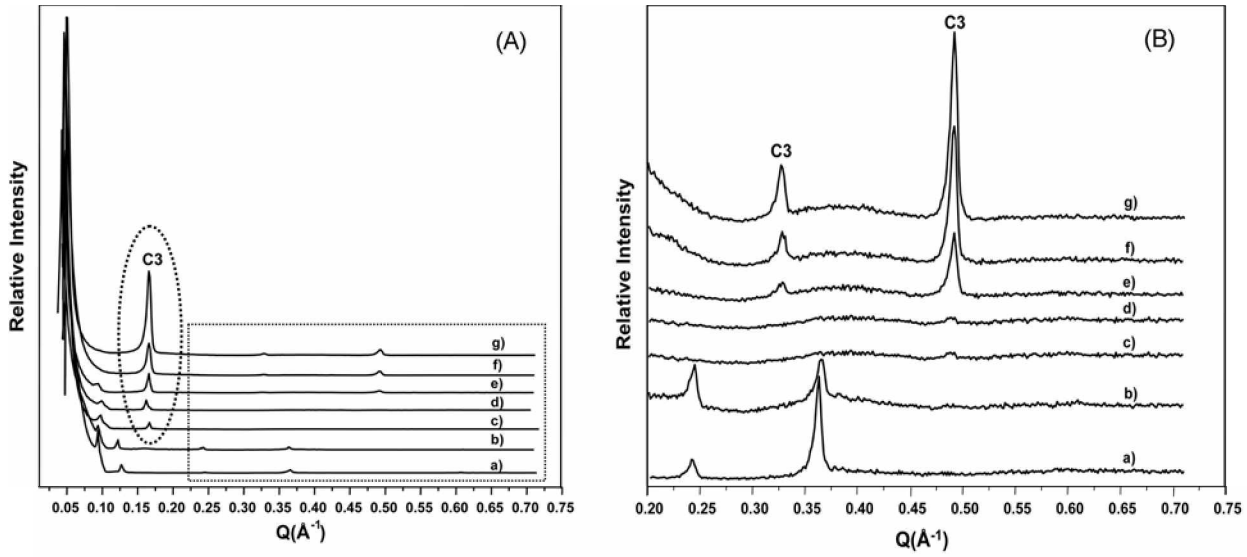

Figure 4. SAXS patterns of DSPC lamellar crystalline phases swollen by an excess of PG depending on the variance of CER3 at 24 °C ± 1 °C below overall transition temperature (T_c): DSPC was fixed at 20.0% w/w and PG was variable correspondingly to increasing the content of CER3. a) 1.0% w/w CER3, b) 2.0% w/w CER3, c) 3.0% w/w CER3, d) 5.0% w/w CER3, e) 7.0% w/w CER3, f) 10.0% w/w CER3, g) 15.0% w/w CER3.

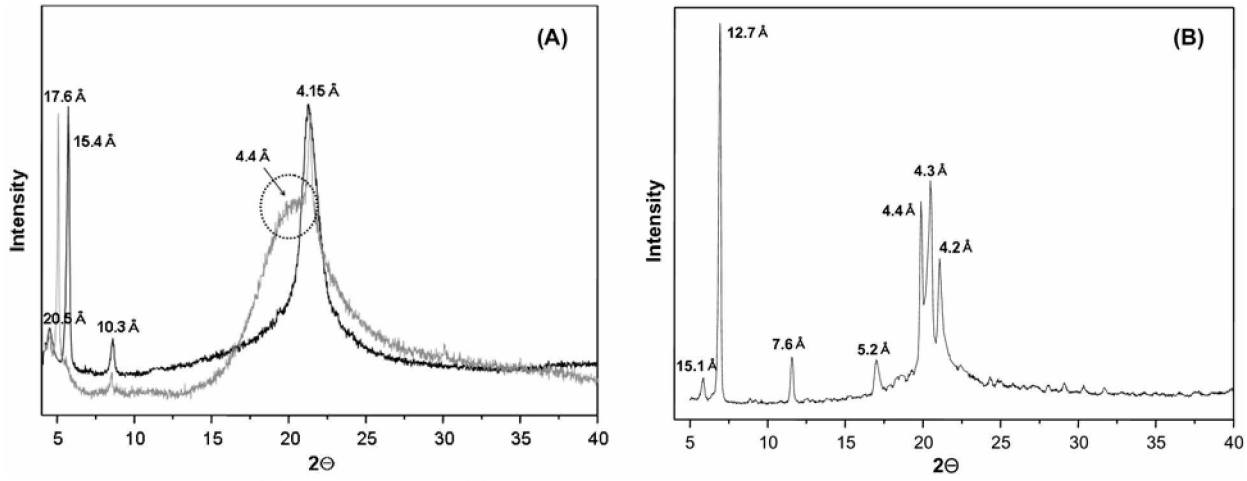

Figure 5. Wide angle X-ray diffraction patterns (A) for DSPC itself (Black line) and its complex (Gray line) swollen by an excess of PG (DSPC:PG = 20 wt%:80 wt%), and (B) for CER3 itself.

2θ = 21.24° dominated the wide angle X-ray diffraction (WAXD) pattern. The high intensity peak obtained from the WAXD pattern corresponds to the electron dense phosphate fragments in the head groups of DSPC. However, the inducement of PG into DSPC made another diffused peak appear beside the dominated peak in the region of 2θ = 20.2° and this diffused or broad peak arises from the electron density contrast between the bilayer and the solvent such as PG[28] In the previous study, the influence of PG incorporated into DSPC has ever been investigated.[12]

Experimentally, CER3 to be used in this study showed the WAXD pattern to have 6 characteristic peaks at 2θ = 5.84°, 6.94°, 11.56°, 16.94°, 19.88°, 20.46°, and 21.08°. The interlayer distance(d) between bilayers is possible to be calculated from the intensity maxima as a dominated peak by following equation (1) below: d = interlayer distance, λ = wave length of X-ray (1.54 Å), 2θ = Bragg's angle

$$d = \lambda/(2\sin\theta) \quad (1)$$

Following the above, the interlayer distance (d) between bilayers could be calculated and each d value was shown in Figure 5.

In Figure 6, it was shown that the incorporation of CER3 into DSPC lamellar phase made the overall structural conformations (Fig. 6(A)) in the measuring range and the regional patterns (Fig. 6(B)) in 2θ values from 4° to 10°, changed with increasing CER3 contents with WAXD. In the range of CER3 content up to 2 wt%, there were no characteristic peaks correspondingly to both of DSPC and CER3 except the main peaks and another diffused peaks at 2θ = 5.5 ± 0.4° appeared by overlapping two peaks for both DSPC at 2θ = 5.72° and CER3 at 2θ = 5.84°. These results suggest that CER3 was well incorporated into DSPC lamellar phase swollen by PG and formed the homogeneous lamellar structure being composed of DSPC and CER3.

However, from 3.0 wt% of CER3, two characteristic diffractions of CER3 appeared again at 2θ = 6.94°, 11.56° and their intensities were dramatically elevated with the increase of CER3, while the characteristic diffraction of DSPC also emerged at 2θ = 4.3°. At the same time, the intensity of the diffused diffraction at 2θ = 5.5 ± 0.4° was shown to be gradually stronger with the similar aspect to other diffractions. From these results, it can be estimated that increasing CER3 to be incorporated into DSPC lamellar phase is continuous to form the miscible lamellar phase together, but simultaneously excess of CER3 becomes immiscible with DSPC to be separated from the DSPC-CER3 lamellar phase and they form separated lamellar crystalline phases, respectively.

Thermal transitions corresponding to the increase of CER3 by DSC: Figure 7 shows the thermal transitions of the model matrices depending upon the CER3 contents. The CER3 showed the transition temperature at 98.98 °C and the enthalpy change (ΔH) of 93.35 J/g which is higher than the ΔH (44.6 J/g) of DSPC and can be inferred to have a higher crystallinity than DSPC.

As shown in Figure 7, the model matrices in a low level of CER3 showed the monotectic thermal transitions, while the model matrices above a certain level of CER3 showed weak eutectic thermal transitions which correspond to the main lamellar phase being composed of DSPC/CER3 and the separated CER3 crystalline phase swollen by PG respectively. Increasing up to 3 wt% of CER3, the model matrices showed the monotectic thermal transitions and these results explain that CER3 molecules are compatible with DSPC to form the homogeneous and well-packed LC matrices due to

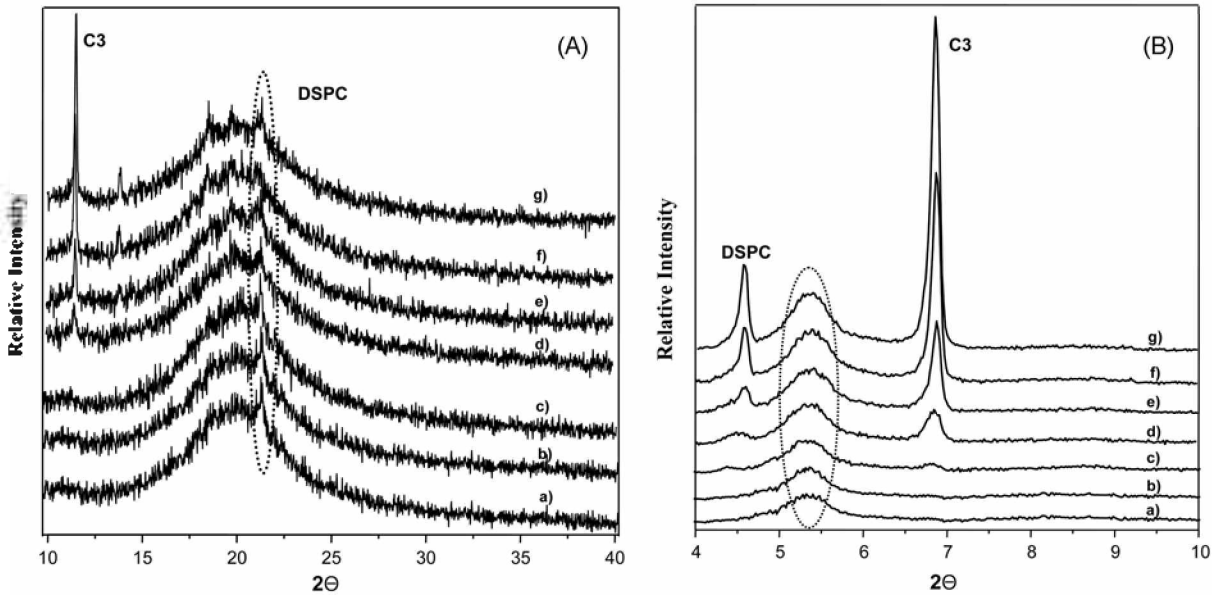

Figure 6. WAXS patterns of DSPC lamellar crystalline phases swollen by an excess of PG depending on the variance of CER3 at 24 °C ± 1 °C below overall transition temperature (T_c): DSPC was fixed at 20.0% w/w and PG was variable correspondingly to increasing the content of CER3. a) 1.0% w/w CER3, b) 2.0% w/w CER3, c) 3.0% w/w CER3, d) 5.0% w/w CER3, e) 7.0% w/w CER3, f) 10.0% w/w CER3, g) 15.0% w/w CER3.

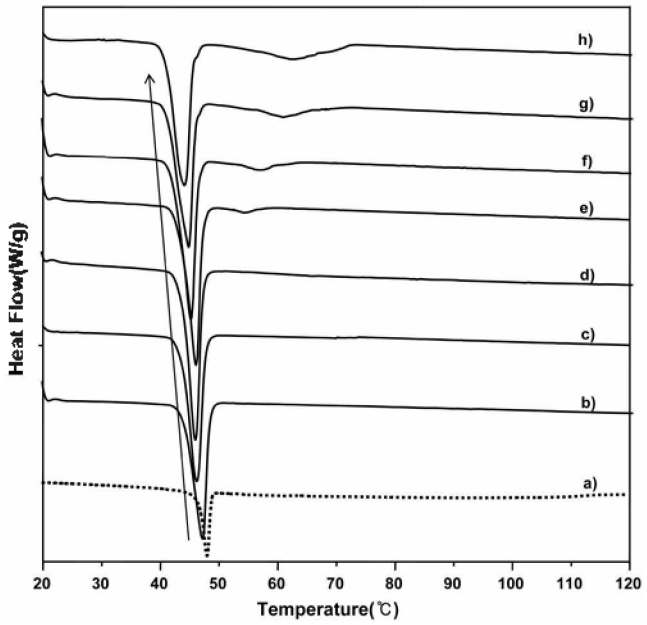

Figure 7. DSC curves of lamellar crystalline phases for each model matrix depending on the variance of CER3 during heating process from 20 ℃ to 120 ℃: DSPC was fixed at 20.0% w/w and PG was variable correspondingly to increasing the content of CER3: a) 0% w/w: 47.93 ℃, 10.31 J/g, b) 1.0% w/w: 47.27 ℃, 16.86 J/g, c) 2.0% w/w: 46.43 ℃, 17.2 J/g, d) 3.0% w/w: 46.20 ℃, 17.45 J/g, e) 5.0% w/w: 46.20 ℃, 18.12 J/g, f) 7.0% w/w: 45.29 ℃, 18.72 J/g, g) 10.0% w/w: 44.84 ℃, 19.11 J/g, h) 15.0% w/w: 44.16 ℃, 19.65 J/g.

their structural similarities.

More increasing over 3 wt% of CER3, they showed the eutectic thermal transitions and the second transition temperature (T_{C2}) was gradually shifted to higher temperature (54.2 ℃ to 63.3 ℃) depending upon the CER3 content. Therefore, it was confirmed that some portion of CER3 was separated from the main lamellar phase and formed the CER3 crystalline phase swollen by PG. These results were almost in accordance with the above results from XRDs.

As seen in Figure 8(A), increasing CER3, it showed the main transition temperatures (T_{C1}) to be gradually decreased from 47.93 ℃ to 44.16 ℃ and it suggests that three hydroxyl groups of CER3 enhance the swollen effect of these lamellar structures by a polar group interaction with PG molecules. On the other hand, as shown in Figure 8(B), increasing CER3, the enthalpy change (ΔH) to be significantly increased from 10.31 J/g to 16.86 J/g even by incorporating only 1 wt% of CER3 and then be gradually increased. This result suggests that CER3 molecule has a relatively higher ΔH than DSPC by its higher crystallinity and the incorporated CER3 molecules into DSPC lamellar phase make the model matrices more dense and thicker. These results were shown to be in good agreement with PM photographs in Figure 9.

As seen in Figure 9, increasing CER3, PM images showed the larger formation of the crystalline phases and this is the reason why CER3 has a higher crystallinity than DSPC and a structural similarity to DSPC enough to be well-packed in these model matrices, and therefore, incorporating CER3 made the formation of the lamellar phases larger, in spite of being more swollen by PG. Also, from 5 wt% of CER3, the formation of separated CER3 crystalline phases started and it seemed to show the larger formation of the crystalline phases, because it was very difficult to differentiate both crystalline phase in PM study.

The micro-structural variances of the model matrices depending on the CHOL contents at a fixed 20 wt% of DSPC

Structural transitions corresponding to the increase of CHOL by XRDs: Experimentally, CHOL used in this study showed the SAXD pattern to have a single crystalline lamellar phase at q = 0.186, 0.369, 0.570 $Å^{-1}$ (the average distance adding up at these q values was calculated as 33.60

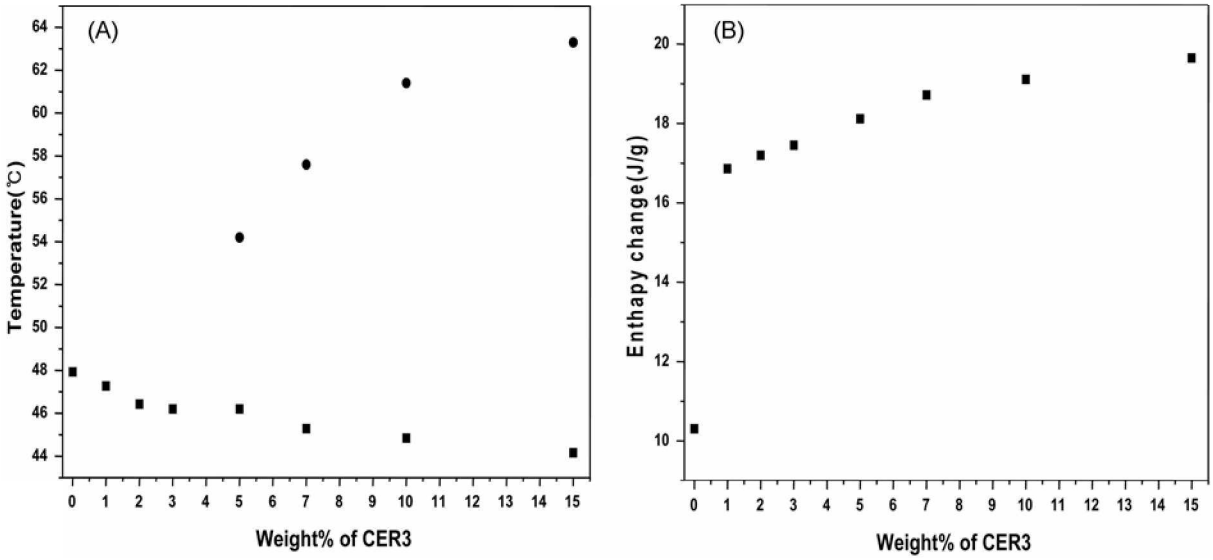

Figure 8. Variances of (A): phase transition temperatures (T_{c1}, ■ and T_{c2}, ●), and (B): enthalpy change (ΔH, ■) at each T_{c1}, depending on CER content.

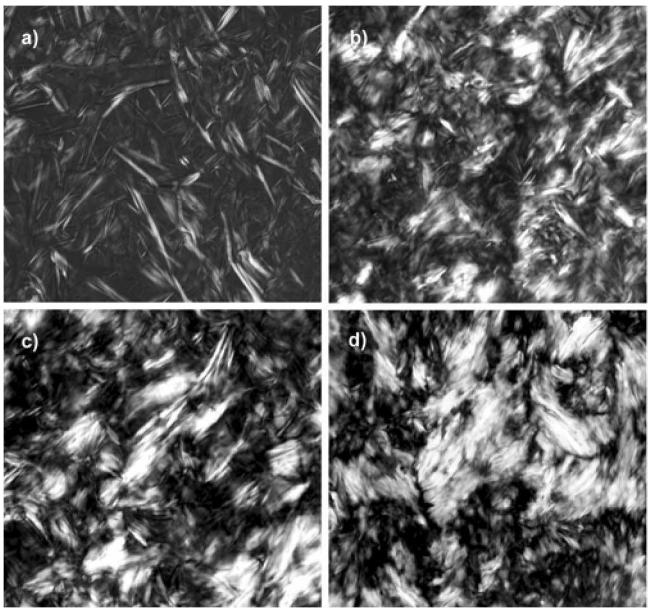

Figure 9. PM photographs (× 1,000 magnification) of lamellar crystalline phases for each model matrix depending on the variance of CER3 contents.: DSPC was fixed at 20.0% w/w and PG was variable correspondingly to increasing the content of CER3: a) 0% w/w, b) 3.0% w/w, c) 5.0% w/w, d) 7.0% w/w.

Å which is almost same distance as Gomez- Fernandez *et al.*[29]). There were no characteristic LPP diffractions for both DSPC and CHOL, but. interestingly, the formation of the characteristic LPP was appeared as soon as CHOL was incorporated into the DSPC/PG lamellar phase as well as the characteristic SPP. similarly to the inducement by CER3.

As seen in Figure 3, CHOL has a bulky molecular structure very differently from DSPC and a high crystallinity. In Figure 10. it was shown that the incorporation of CHOL into DSPC lamellar phase made the overall structural transitions (Fig. 10(A)) in the measuring range and the regional transition patterns (Fig. 10(B)) in q values from 0.1 to 0.75. dependently on increasing the CHOL content with SAXD. There were three peaks representing for LPP at q = 0.054 $Å^{-1}$, 0.108 $Å^{-1}$. and 0.169 $Å^{-1}$ and the distance of LPP at these q values was calculated as approximately 114.6 Å. while two types of SPP were emerged: one diffraction represents for DSPC at q = 0.232 $Å^{-1}$ and another diffraction represents for CHOL at q = 0.181 $Å^{-1}$, 0.359 $Å^{-1}$. In Figure 10(A). (B). even though only 1 wt% of CHOL is incorporated into DSPC lamellar phase, the characteristic peaks of CHOL at q = 0.181 $Å^{-1}$. 0.359 $Å^{-1}$ appeared and it means the existence of crystalline CHOL due to the immiscibility of CHOL with DSPC swollen by PG differently from CER3.

Also, more increasing CHOL, the intensity of the 1st order diffraction for LPP was gradually weakened in Figure 10(A), and the intensities of the characteristic diffractions for DSPC at q = 0.130 $Å^{-1}$, 0.254 $Å^{-1}$ were also remarkably weakened in Figure 10(B). Therefore, these results describe that the incorporation of CHOL gradually broadens the DSPC lamellar structure due to its bulky chemical structure caused by several cyclic rings and inhibits the formation of the dense lamellar phase, as well as giving the membrane fluidity to it. Contrarily. the intensity of the characteristic diffraction for CHOL at q = 0.181 $Å^{-1}$ was dramatically strengthened with increasing CHOL due to its high crystallinity while another one at q = 0.359 $Å^{-1}$ almost was not changed.

Experimentally, CHOL used in this study showed much more complex WAXD pattern to have quite many tiny peaks than CER3, but the dominant peaks could be differentiated as 7 peaks and these peaks were found at 2θ = 5.24°, 14.44°, 15.3°, 17.34°, 18.08°, 20.1°, and 21.38° (Data was not shown).

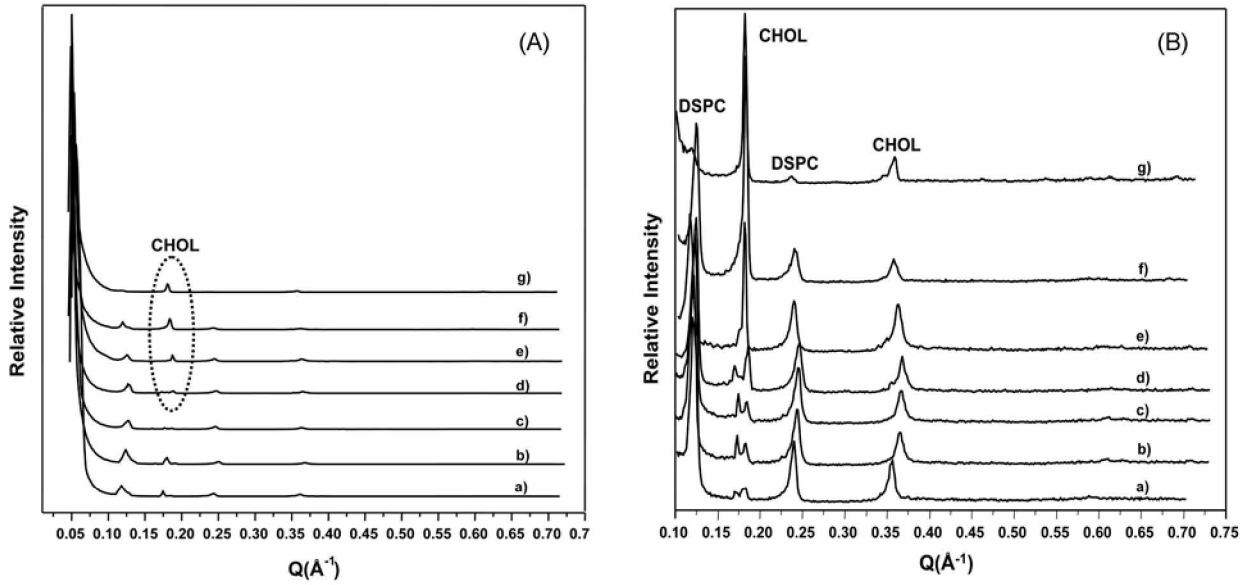

Figure 10. SAXS patterns of DSPC lamellar crystalline phases swollen by an excess of PG depending on the variance of CHOL at 24 °C ± 1 °C below overall transition temperature (T_c): DSPC was fixed at 20.0% w/w and PG was variable correspondingly to increasing the content of CHOL. a) 1.0% w/w CHOL, b) 1.5% w/w CHOL, c) 2.0% w/w CHOL, d) 2.5% w/w CHOL, e) 3.0% w/w CHOL, f) 5.0% w/w CHOL, g) 10.0% w/w CHOL.

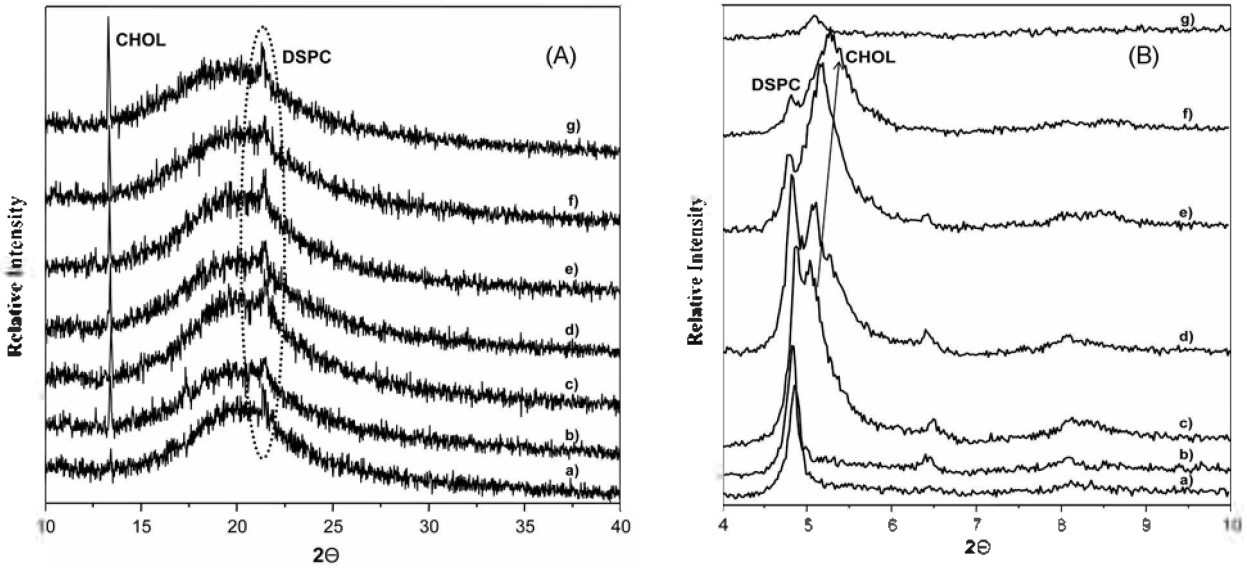

Figure 11. WAXS patterns of DSPC lamellar crystalline phases swollen by an excess of PG depending on the variance of CHOL at 24 °C ± 1 °C below overall transition temperature (T_c): DSPC was fixed at 20.0% w/w and PG was variable correspondingly to increasing the content of CHOL. a) 1.0% w/w CHOL, b) 1.5% w/w CHOL, c) 2.0% w/w CHOL, d) 2.5% w/w CHOL, e) 3.0% w/w CHOL, f) 5.0% w/w CHOL, g) 10.0% w/w CHOL.

In Figure 11, it was shown that the incorporation of CHOL into DSPC lamellar phase made the overall structural conformations (Fig. 11(A)) in the measuring range and the regional patterns (Fig. 11(B)) in 2θ values from 4° to 10°, changed with increasing CHOL contents with WAXD. As seen in Figure 11(A), among them, three peaks at 2θ = 17.34°, 18.08°, and 20.1° were easy to be diffused in the presence of DSPC, and so their usefulness in detecting the formation of separated CHOL crystalline phase is somewhat limited, similarly in Bach *et al.*'s study.[30] In the same way as the SAXD results, even though only 1 wt% of CHOL is incorporated into DSPC lamellar phase, the characteristic peak of CHOL at 2θ = 13.4° slightly shifted to the left side appeared and the intensity was also gradually strengthened dependently upon increasing the CHOL content and it indicates the onset forming crystalline CHOL by above reason of the immiscibility of CHOL.

In Figure 11(B), another peak at 2θ = 4.9° appeared to be slightly shifted to the right side by overlapping two peaks for both DSPC at 2θ = 4.30° and CHOL at 2θ = 5.24° up to 1.5 wt% of CHOL. From 2.0 wt% to 5.0 wt% of CHOL, this overlapped diffraction was started to be distinctively divided by two characteristic peaks for DSPC and CHOL due to increasing their immiscibility. Moreover, one diffraction for DSPC at $2\theta = 4.7 \pm 0.1$° became proportionally weakened dependently upon increasing CHOL, and correspondingly, another diffraction for CHOL at $2\theta = 5.2 \pm 0.2$° was not significantly changed in their intensities and was observed only to be little shifted to the right side. Much more increasing CHOL to 10 wt%, the diffraction for DSPC completely disappeared and it suggests that this lamellar system was almost broken down due to its bulky molecular structure. These above results suggest that CHOL alone was so difficult to be completely incorporated into DSPC lamellar phase swollen by PG and was easy to be separated to form CHOL crystalline phase even in its small level or break the lamellar structure down in its extremely high level.

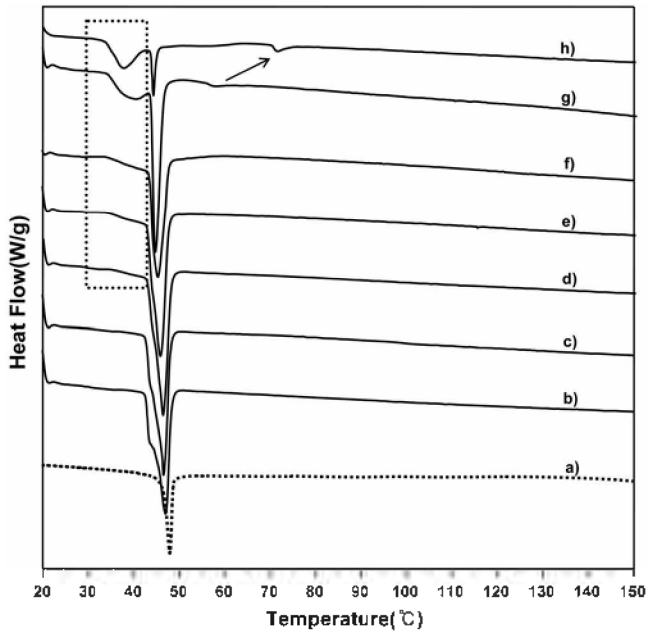

Figure 12. DSC curves of lamellar crystalline phases for each model matrix depending on the variance of CHOL during heating process from 20 °C to 150 °C: DSPC was fixed at 20.0% w/w and PG was variable correspondingly to increasing the content of CHOL.: a) 0% w/w, b) 1.0% w/w, c) 1.5% w/w, d) 2.0% w/w, e) 2.5% w/w, f) 3.0% w/w, g) 5.0% w/w, h) 10.0% w/w.

Thermal transitions corresponding to the increase of CHOL by DSC: CHOL used in this study showed the transition temperature at 147.5 °C and the enthalpy change (ΔH) of 78.61 J/g(the data was not shown). As seen in

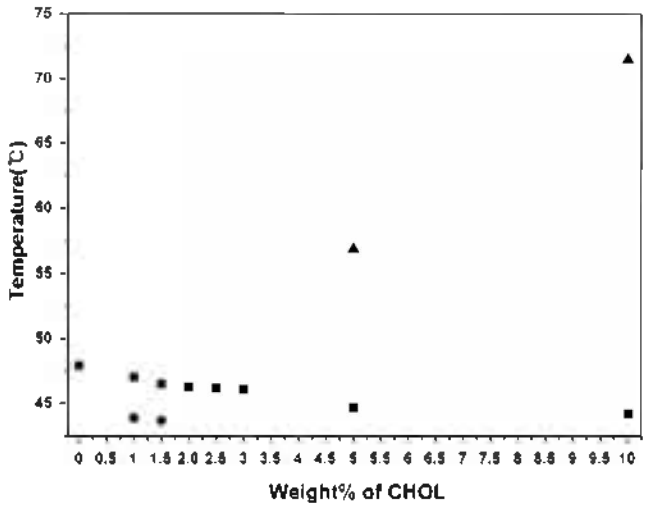

Figure 13. Variances of the phase transition temperatures (T_{c1}, ■, T_{c2}, ○, and Tc3, ▲) depending on CHOL content.

Figure 12 and Figure 13, all model matrices which CHOL was incorporated showed the eutectic thermal transitions and the main transition temperature (T_{c1}) wholly shifted to slightly lower temperature from 47.93 °C to 44.31 °C with increasing CHOL content. but their transitional behaviors were quite different dependently upon the CHOL level. Because of the overlapped and complicated behaviors in Figure 12, the enthalpy changes (ΔHs) for most model matrices could not be exactly calculated.

In the range of CHOL to 1.5 wt%, the eutectic thermal transitions were observed as the closely overlapped aspects of the main lamellar phase (T_{c1}) with the CHOL-rich phase (T_{c2}) in the presence of PG. From 2.0 wt% of CHOL to 3.0 wt%. those transitions started to be separated from the main transition and more increasing CHOL to 5 wt% made the CHOL-rich phase be more distinctive and then increasing to 10 wt%, this transition got to be definitely distinguished from the main transition.

Also, from 5 wt%, another sub-transition emerged at higher temperature (56.8 °C) corresponding to the separated CHOL crystalline (T_{c3}) phase swollen by PG and increasing to 10 wt%, this transition shifted to much higher temperature (71.36 °C) as well as be more apparent. The formation of separated CHOL crystalline phase was also observed by PM photographs (Fig. 14).

From the above results. it can be explained that CHOL molecules alone are not compatible with DSPC in the presence of excess PG. and make DSPC-based lamellar structure loosened at small level due to its bulky molecular structure and totally destroyed at higher level due to its high crystallinity. while there were other two coexisting crystalline phases correspondingly to the main lamellar phase and the separated CHOL crystalline phase, likely to the results observed by PM. In Figure 14. most of samples were observed by 1,000 times of magnification. but at 10 wt% of CHOL, it was difficult to be observed by 1.000 times of magnification and it couldn't afford to be done by 400 times of magnification. As seen in Figure 14, increasing the CHOL content, the rod-like CHOL crystalline phase was shown to be gradually more apparent. and simultaneously the main lamellar phase was shown to be gradually less apparent and seemed to be almost disappeared at 10 wt% of CHOL.

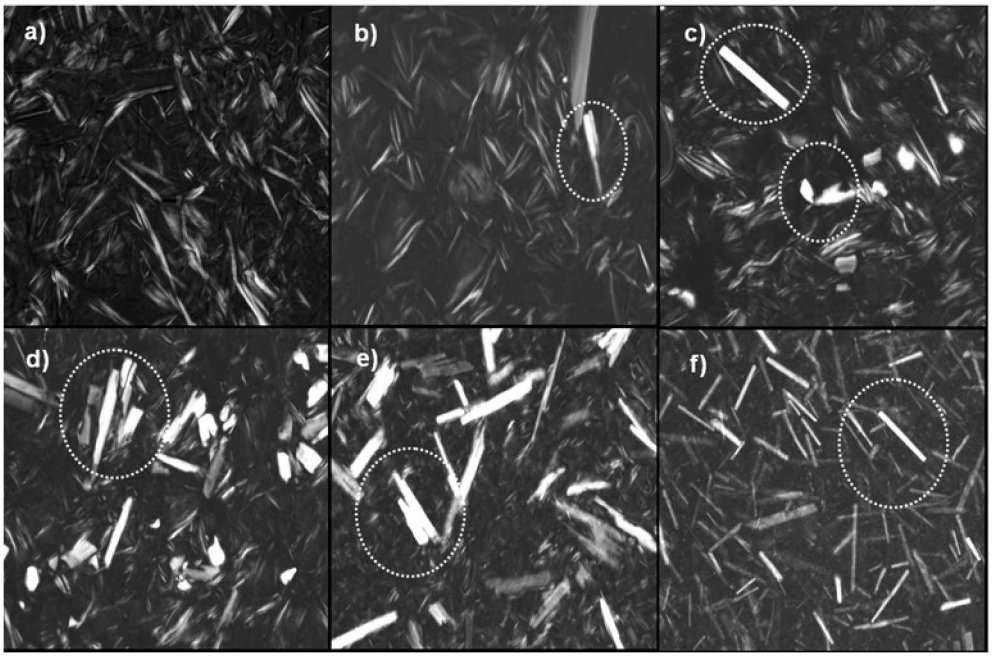

Figure 14. PM photographs of lamellar crystalline phases for each model matrix depending on the variance of CHOL:DSPC was fixed at 20.0% w/w and PG was variable correspondingly to increasing the content of CHOL: a) 0% w/w (× 1,000), b) 1.0% w/w (× 1,000), c) 3.0% w/w (× 1,000), d) 5.0% w/w (× 1,000), e) 7.0% w/w (× 1,000), f) 10.0% w/w (× 400).

Conclusions

In the previous study, we have ever investigated the lyotropic and thermotropic behaviors of DSPC-based lamellar liquid crystal swollen by PG as a polar solvent without water to stably encapsulate retinoids, ubiquinones, tocopherols etc. by avoiding the contact with water molecules and protect from their oxidization.

In this study, in order to design the model matrix which is more similar structure to human SC and has better skin affinity, we investigated the influence of CER3 and CHOL as other lipids in human SC on a non-hydrous DSPC-based lamellar structure with DSC, SAXD, WAXD, and PM. CER3 molecules play a very important role to form the LPP as well as the SPP similar to human SC, while it makes the model matrices more dense and thicker.

Incorporating small amounts of CER3, it could form the homogeneous lamellar phase with DSPC in the presence of excess PG due to its similar molecular structure to DSPC and it could be explained by that there were no characteristic peaks of CER3 from XRDs and DSC results also showed the monotectic thermal transitions and the elevated enthalpy changes (ΔHs). However, more increasing the CER3 content, the characteristic diffractions for CER3 emerged and their intensities were dramatically strengthened from XRDs and DSC results showed the eutectic thermal transitions which T_{e2} shifted to higher temperatures and these results were caused by the formation of separated CER crystalline phase due to its high crystallinity and immiscibility with DSPC.

Differently from CER3, incorporating even small amounts of CHOL, the characteristic diffractions for CHOL emerged and their intensities were dramatically strengthened from XRDs, while the intensities of characteristic diffractions for DSPC was gradually weakened due to its bulky molecular structure. DSC results also showed the eutectic thermal transitions which are more complex than CER3 and these results were caused by the formation of CHOL-rich lamellar phase and separated CHOL crystalline phase due to its high crystallinity and immiscibility with DSPC.

In order to make these non-hydrous model matrices similar to human SC, it is needed to more investigate for the desirable composition among these lipids and incorporate other lipids such as fatty acids and oils to help transdermal drug delivery in the application of cosmetics and pharmaceutics. Therefore, in a forthcoming paper, the study for the desirable composition among DSPC, CER3, CHOL will be discussed in the presence of PG without water.

References

1. Wertz, P. W.; Downing, D. T. *Stratum Corneum: Biological and Biochemical Considerations* in *Transdermal Drug Delivery*; Hadgraft, J.; Guy, R. H., Eds.; Marcel Dekker: New York, 1989; pp 1-17.
2. Potts, R. O.; Guy, R. H. *Pharm. Res.* **1992**, *9*, 663.
3. Storm, G.; Oussoren, C.; Peeters, P. A. M. *Safety of Liposome Administration* in *Membrane Lipid Oxidation*; Vigo-Pelfrey, C., Ed.; CRC press: Boca Raton, FL, 1991; Vol. III, p 239.
4. Becher, P. *Emulsion: Theory and Practice*; R. E. Krieger Publishing: Malabar, FL, 1985.
5. Davis, S. S.; Hadgraft, J.; Palin, K. J. In *Encyclopedia of Emulsion Technology*; Becher, P., Ed.; 1983; Vol 2, p 159.
6. Barry, B. W. *J. Control. Release* **1987**, *6*, 85.
7. Sheth, N. V.; Freeman, D. J.; Higuchi, W. I.; Spruance, S. L. *Int. J. Pharm.* **1986**, *28*, 201.
8. Nicolazzo, J. A.; Morgan, T. M.; Reed, B. L.; Finnin, B. C. *J. Controlled Release* **2005**, *103*, 577.
9. Lim, P. F. C.; Liu, X. Y.; Kang, L.; Ho, P. C. L.; Chan, Y. W.; Chan, S. Y. *Int. J. Pharm.* **2006**, *311*, 157.
10. Fang, J. Y.; Hwang, T. L.; Leu, Y. L. *Int. J. Pharm.* **2003**, *250*, 313.
11. Bonina, F. P.; Carelli, V.; Colo, G. D.; Montenegro, L.; Nannipieri, E. *Int. J. Pharm.* **1993**, *100*, 41.
12. Jeong, T. H.; Oh, S. G. *Bull. Korean Chem. Soc.* **2007**, *28*, 108.
13. Elias, P. M. *J. Invest. Dermatol.* **1983**, *80*, 213.
14. Elias, P. M.; Goerke, J.; Friend, D. S. *J. Invest. Dermatol.* **1977**, *69*, 535.
15. Lampe, M. A.; Williams, M. L.; Elais, P. M. *J. Lipid Res.* **1983**, *24*, 120.
16. Elias, P. M. *The Importance of Epidermal Lipids for the Stratum Corneum Barrier* in *Topical Drug Delivery Formulation*; Osborne, D. W., Amann, A. H., Eds.; Marcel Dekker Inc: New York and Basal, 1989; pp 13-28.
17. Wertz, P. W. *Adv. Drug Deliv. Rev.* **1996**, *18*, 283.
18. Wertz, P. W.; Miethke, M. C.; Long, S. A.; Strauss, J. S.; Downing, D. T. *J. Invest. Dermatol.* **1985**, *84*, 410.
19. Robson, K. J.; Stewart, M. E.; Michelsen, S.; Lazo, N. D.; Downing, D. T. *J. Lipid Res.* **1994**, *35*, 2060.
20. Stewart, M. E.; Downing, D. T. *J. Lipid Res.* **1999**, *4*, 1434.
21. Ponec, M.; Weerheim, A.; Lankhorst, P.; Wertz, P. *J. Invest. Dermatol.* **2003**, *120*, 581.
22. Mouritsen, O. G.; Jorgsesen, K. *Chem. Phys. Lipids* **1994**, *73*, 3.
23. Ipsen, J.; Karlstrom, G.; Mouritsen, O.; Wennerstrom, H.; Zuckermann, M. *Biochim. Biophys. Acta* **1987**, *905*, 162.
24. Moore, D. J.; Rerek, M. E. *Acta Derm. Venereol. Suppl.* **2000**, *208*, 16.
25. Zbytovska, J.; Kiselev, M. A.; Funari, S. S.; Garamus, V. M.; Wartewig, S.; Neubert, R. *Chemistry and Physics of Lipids* **2005**, *138*, 69.
26. Bouwstra, J. A.; Gooris, G. S.; van der Spek, J. A.; Bras, W. *J. Invest. Dermatol.* **1991**, *97*, 1005.
27. de Jager, M. W.; Gooris, G. S.; Dolbnya, I. P.; Bras, W.; Ponec, M.; Bouwstra, J. A. *Chem. Phys. Lipids* **2003**, *124*, 123.
28. Glatter, O.; Kratky, O. *Small Angle X-Ray Scattering*; Academic Press: New York, 1982.
29. Jimenez-Monreal, A. M.; Villalain, J.; Aranda, F. J.; Gomez-Fernandez, J. C. *Biochim. Biophys. Acta* **1998**, *1373*, 209.
30. Bach, D.; Wachtel, E. *Biochim. Biophys. Acta* **2003**, *1610*, 187.